



Thermoreversible helical fibers from photoreactive triphenylene-derived liquid crystals in liquid paraffin

Takuji Hirose^a, Yuka Kikuchi^a, Tomoaki Nakano^a, Tsukasa Ohno^a, Kengo Kawamura^a, Normazliana Binti Nazri^b, Atsuhiko Fujimori^a, Koichi Kodama^{a,*}, Mikio Yasutake^a

^a Graduate School of Science and Engineering, Saitama University, 255 Shimo-ohkubo, Sakura, Saitama, 338-8570, Japan

^b Department of Applied Chemistry, Saitama University, 255 Shimo-ohkubo, Sakura, Saitama, 338-8570, Japan

ARTICLE INFO

Keywords:

Triphenylene-derived liquid crystal
Photocyclization reaction
Helical fiber
Assembly
Thermal reversibility

ABSTRACT

Liquid crystalline triphenylene derivatives, **TPC1_p-n** (n = 6, 12, 14, 16) were prepared using *p*-alkoxycinnamate as the [2+2] photo-cyclization site. **TPC1_p-n** (n = 12, 14, 16) showed Col_r phase and gave crescent-shaped or helical fibers after UV-irradiated in liquid paraffin solutions at 90 and 110 °C in the Col_r temperature range. The apparent photoreaction products were shown to be thermally reversible, i.e. they dissolved in liquid paraffin at high temperatures and reappeared on cooling, indicating that they were aggregates of oligomerized **TPC1_p-n**. The reaction mechanism was discussed in terms of the structure of the liquid crystalline phase.

1. Introduction

The self-assembly of organic molecules is a focus in the materials science field in terms of electronic devices, photonic devices, and so on [1–7]. From low molecular weight compounds to macromolecules, liquid crystalline (LC) compounds are attractive self-organizing soft materials that exhibit both fluidity and order, depending on the environments. In addition to flat panel displays, LC materials are studied as various functional materials. The functions expected from ordered structures are diverse such as charge energy transport, optical function, recognition and separation as reported by many studies [8–11]. Fluidity is important to help improve productivity and the uniformity of its products. Studies on LC materials, therefore, are promoted to understand the basic properties and to realize various forms of integrated structures from one-dimensional (1D) to three-dimensional (3D), fibrous to sheet-like, and tubular ones [5–8]. Numerous type molecules have been designed and synthesized by using different constituent atoms, bonds, and functional groups.

Discotic LC compounds belong to a unique category of LC compounds, where the most interesting feature is the construction of one-dimensional columnar structures [4,7–21]. To exploit this feature, charge and heat transport is one of the main application topics being studied [4,7,10,12–18], and applications to recognition and separation seem to be specific to 1D columnar structures [8,9,11,20,21]. More recently, more elaborate and interesting systems have been developed to construct basal discs from multiple molecules [8,11,17,18,20]. Nevertheless, among the many discotic LC systems, those derived from triphenylene derivatives have not only been the most widely studied to date, but also continue to be explored for their novel chemical structure-columnar geometry relationships [21,22] and applications [4,12,18,19]. With the aim of retaining their 1D columnar structure and function, several reactions have been applied

* Corresponding author.

E-mail address: kodama@mail.saitama-u.ac.jp (K. Kodama).

<https://doi.org/10.1016/j.heliyon.2023.e22037>

Received 18 August 2023; Received in revised form 29 October 2023; Accepted 2 November 2023

Available online 10 November 2023

2405-8440/© 2023 The Authors. Published by Elsevier Ltd. This is an open access article under the CC BY-NC-ND license (<http://creativecommons.org/licenses/by-nc-nd/4.0/>).

to covalently link triphenylene derivatives. Most of them are polymerization reactions [8,10,11] and cross-linking reactions [12,19,20] of the peripheral end groups.

We developed photoreactive columnar LC compounds and investigated the effect of UV irradiation in liquid paraffin with no additives at the temperature in LC state [23]. They were triphenylene derivatives, **TPC1_p-n** and **TPC2_{mp}-n** (Fig. 1), with six cinnamate units with one or two linear alkoxy groups ($C_nH_{2n+1}O$; $n = 10-14$) as peripheral groups, respectively. **TPC2_{mp}-n** underwent a photocrosslinking reaction when irradiated with UV light in liquid paraffin at $\sim 100^\circ\text{C}$, which is in the Col_h temperature range, and transformed into linear fibrous products up to 2 mm long. A brief examination of **TPC1_p-n** ($n = 10, 12, 14$) also showed that they form fiber-like structures in the Col_r temperature range. In this study, further examination of **TPC1_p-n** ($n = 12, 14, 16$) revealed that their fibrous products were thermoreversible. Considering the effect of length and number of peripheral chains, the expected photoreaction mechanism is discussed.

2. Results and discussion

2.1. Thermal properties of **TPC1_p-n** ($n = 6, 16$)

Two new triphenylene derivatives, **TPC1_p-n** ($n = 6, 16$), were prepared from hexahydroxytriphenylene and the corresponding substituted cinnamic acid chloride following the previous procedure [23]. The optical textures were studied by polarized optical microscopy (POM), and the phase transition temperatures and the heats of phase transition were determined by differential scanning calorimetry (DSC). For the LC phase determination, X-ray diffraction (XRD) was performed by changing the temperature. The phase transition behaviors are summarized in Table 1 with those of **TPC1_p-n** ($n = 12, 14$) reported previously [23]. From the DSC measurements of **TPC1_p-6**, an endothermic change was observed at 166°C on the heating process as seen in Table 1. From the POM observation (Fig. S1a) and the XRD profiles (Fig. S2), it was shown that the change is the crystal-nematic LC phase transition as the schlieren texture was observed. The crystalline phase should be caused by its shorter alkoxy chains. On the other hand, the LC phase above 90°C of **TPC1_p-16** was shown to be a rectangular columnar phase, Col_r , from the mosaic texture (Fig. S1b) and the XRD data analysis (Fig. S3a and Table S1). At lower temperature than 70°C , **TPC1_p-16** seems to be a glassy state from the XRD profile (Fig. S3b) but the glassy state-LC state transition was not clearly determined from the DSC measurement as in the case of **TPC1_p-n** ($n = 12, 14$) (Table 1). The phase transition temperature in a square blanket was determined by the POM observation but the discotic nematic-isotropic phase transition could not be determined either by DSC measurements or by POM observations.

2.2. UV irradiation of **TPC1_p-n** in liquid paraffin

The solubility of **TPC1_p-n** ($n = 6, 12, 14, 16$) in liquid paraffin was examined. **TPC1_p-6** did not dissolve at temperatures up to 120°C well below the crystal-LC transition temperature, while the others dissolved to clear solutions at around 90°C . When the temperature was lowered below $40-50^\circ\text{C}$, the solutions of **TPC1_p-n** ($n = 12, 14, 16$) became turbid, indicating that aggregation had started due to reduced mobility. These results indicate that liquid paraffin does not have enough interaction to dissolve crystalline triphenylene derivatives and the long linear alkoxy chains, $C_nH_{2n+1}O$ ($n = 12, 14, 16$), contributed to dispersion and dissolution in liquid paraffin.

The effect of UV irradiation in liquid paraffin was studied for **TPC1_p-n** ($n = 12, 14, 16$) at $75, 90,$ and 110°C . The POM photographs were obtained after cooling down to room temperature every 24 h to observe the time course of change and the results are summarized in Table 2 and Table S2.

After UV irradiation at 75°C , granular products were observed in a transparent reaction mixture as shown for **TPC1_p-12** and **TPC1_p-16** in Table 2 (Entries 1 and 2). We infer that they are polymeric materials, poly-**TPC1_p-n** ($n = 12, 14, 16$), formed by [2+2] photocyclization of the cinnamate units. From the thermal property in Table 1, **TPCs** have no good fluidity as a LC state so that granular poly-**TPC1_p-n** was formed due to the photoreaction of amorphous aggregates.

On the other hand, at 110°C , **TPC1_p-n** ($n = 12, 14, 16$) were found to form linear or fibrous products (Table 2, Entries 3–5). The change of the shape should be due to difference of the state of **TPC1_p-n** at the reaction temperatures. The products were prepared by the reaction occurred in 1D direction of the Col_r phase. Almost the same results were obtained at 90°C as shown in Table S2 so that, even at this temperature, the majority of **TPC1_p-n** ($n = 12, 14, 16$) is also considered to be in the columnar phases, respectively (Table 1). An enlarged POM photograph of one fibrous product from **TPC1_p-16** was obtained as shown in Fig. 2a and b. It is helical and resembles yarn made up of short, curved fibers, suggesting the assembly of poly-**TPC1_p-16**. The AFM results shown in Fig. 2c also supports the bundle-like structure of the fibers.

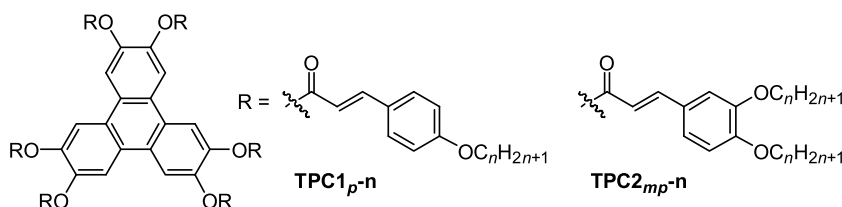


Fig. 1. Structures of triphenylene cinnamate derivatives, **TPC1_p-n** and **TPC2_{mp}-n**.

Table 1
Phase transition behavior of $\text{TPC1}_p\text{-n}$ ($n = 6, 12, 14, 16$) obtained from POM, DSC, and XRD measurements.

compound	Phase transition temperatures ($^{\circ}\text{C}$) and enthalpies (J g^{-1}) ^{a,b}	
	heating	cooling
$\text{TPC1}_p\text{-6}$	Cr 166 (−13.5) N_D –I ^c	I– N_D 139 (12.6) Cr
$\text{TPC1}_p\text{-12}^{\text{d}}$	G [60] ^e Col _r (−0.18) 178 (−1.35) N_D [189] ^e I	I [180] ^e N_D 173 (1.21) Col _r [80] ^e G
$\text{TPC1}_p\text{-14}^{\text{d}}$	G [80] ^e Col _r 197 (−2.76) I	I 193 (1.09) Col _L [90] ^e G
$\text{TPC1}_p\text{-16}$	G [70] ^e Col _r 194 (−1.60) N_D [203] ^e I	I [197] ^e N_D 190 (1.21) Col _r [90] ^e G

^a Determined by DSC ($5^{\circ}\text{C}\cdot\text{min}^{-1}$).

^b Abbreviations: Cr = crystalline phase, N_D = discotic nematic phase, I = isotropic phase, G = glassy phase, Col_r = rectangular columnar phase, Col_L = columnar lamellar phase.

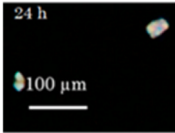
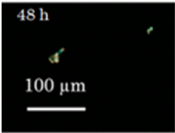
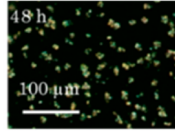
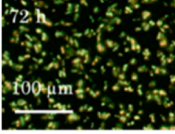
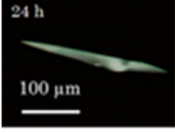
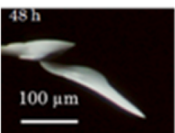
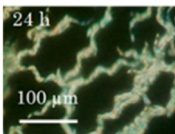
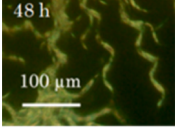
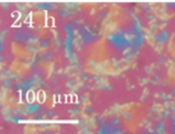
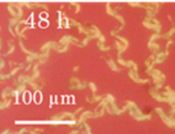
^c Decomposed at $\sim 260^{\circ}\text{C}$.

^d ref. 23.

^e Determined by POM observation.

Table 2

POM observation^a of UV irradiation products of $\text{TPC1}_p\text{-n}$ ($n = 12, 14, 16$) at 75 and $110^{\circ}\text{C}^{\text{b}}$ in liquid paraffin.^c

Entry	TPC (μmol)	Temp ($^{\circ}\text{C}$)	Irradiation time (h)	
			24	48
1	$\text{TPC1}_p\text{-12}$ (0.46)	75		
2	$\text{TPC1}_p\text{-16}$ (0.50)	75		
3	$\text{TPC1}_p\text{-12}$ (0.46)	110		
4	$\text{TPC1}_p\text{-14}$ (0.45)	110		
5	$\text{TPC1}_p\text{-16}$ (0.46)	110		

^a Taken after cooling down to room temperature in cross-polarized light.

^b Reaction temperatures were kept at 75 ± 5 and $110 \pm 5^{\circ}\text{C}$ for 48 h except that, $\text{TPC1}_p\text{-16}$ at 75°C was studied up to 72 h.

^c About 0.5 mg of TPC was irradiated in about 13 mg (1 drop) of liquid paraffin.

The product shapes of $\text{TPC1}_p\text{-12}$ (Table 2, Entry 3), and $\text{TPC1}_p\text{-n}$ ($n = 14, 16$) (Entries 4, 5) differed slightly. $\text{TPC1}_p\text{-12}$ gave more linear crescent-shaped products while from $\text{TPC1}_p\text{-14}$ and $\text{TPC1}_p\text{-16}$, most products were tangled. In fact, sometimes insoluble product from $\text{TPC1}_p\text{-12}$ was obtained as reported previously [23]. As discussed in the section on expected reaction mechanisms below, this may be due to the higher reactivity of $\text{TPC1}_p\text{-12}$ as considering the higher orderliness seen in Fig. S4 comparing to that of $\text{TPC1}_p\text{-16}$

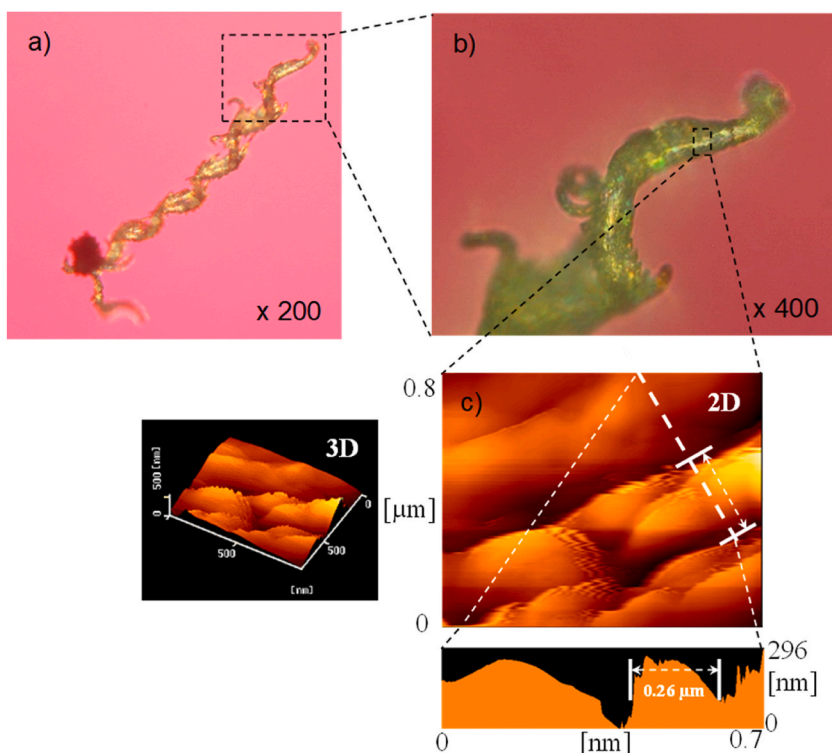


Fig. 2. Enlarged POM ((a) and (b)) and AFM (c) photographs of poly-TPC_{1p}-16.

(Fig. S3).

2.3. Thermal behavior of apparent photoreaction products of TPC_{1p}-n

The reaction products from TPC_{1p}-n ($n = 12, 14, 16$) were thought to dissolve at the reaction temperature, as the shape changed at every observation, that is, dissolution at high temperature and re-emergence when cooled to rt for POM observation. Therefore, it is expected that poly-TPC_{1p}-n has a low degree of polymerization and low degree of cross-linking. Given that the degree of polymerization is low, the size of the apparent products observed in Table 2 is too large and each product should be the result of aggregation of poly-TPC_{1p}-n. In that case, the apparent shape of the product should change depending not only on the UV irradiation conditions, i.e., temperature and time, but also on the cooling process.

The effect of the cooling rate was observed for the solution of the apparent products from TPC_{1p}-14. Fig. 3a shows the result obtained by rapid cooling from 60 °C, which clearly shows an increase in the number of short, curved fibers. On the other hand, as shown in Fig. 3b, when cooling was slowed down to 1 °C/min, thicker and longer fibers appeared. All these results support the formation of helical fiber products by the assembly of short poly-TPCs.

The dissolution and re-assembly process was video-recorded for the apparent photoreaction product from TPC_{1p}-14 in liquid paraffin and is shown in Video S1. When the mixture was warmed, the fibers started to dissolve around 40 °C. When the solution was rapidly cooled from 60 °C on the POM stage, many short fibers appeared. Conversely, when the solution was slowly cooled (0.5 °C/min) and maintained at 30 °C, longer and more helical products appeared.

Supplementary data related to this article can be found online at <https://doi.org/10.1016/j.heliyon.2023.e22037>

The effect of a good solvent of TPC_{1p}-14 was also investigated for the apparent photoreaction products. After UV irradiation, liquid

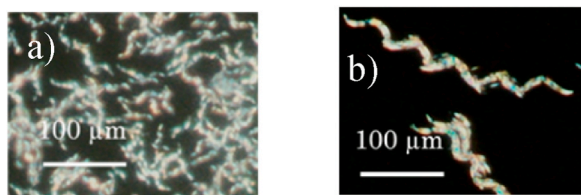


Fig. 3. POM images of poly-TPC_{1p}-14 after a) rapid cooling to room temperature, b) slow cooling with 1 °C/min in liquid paraffin from 60 °C.

paraffin was removed a little and a drop of toluene was added to the reaction mixture at room temperature, and a video was recorded. As shown in **Video S2**, the dissolution of helical fibers proceeded as toluene diffused in liquid paraffin. After some time, fine and short fibers started to appear probably due to evaporation of toluene. Again, this result suggests that the fibers are the assembly of short poly-TPC1_p-14 with low degree of polymerization and cross-linking.

Supplementary data related to this article can be found online at <https://doi.org/10.1016/j.heliyon.2023.e22037>

2.4. Photoreaction mechanism

Based on the photoreaction of TPC1_p-n (n = 12, 14, 16) and the properties of reaction products, the expected mechanism is shown in **Fig. 4**. The TPCs forming the Col_r phase are stacked with the molecular axis inclined to the column axis, as indicated by A. In the previous report [23], it was proposed that [2+2] photocyclization of molecules assembled in the Col_r structures in a film form led to crosslinking and changed to a Col_h-like morphology with overlapping molecules. As polymerization proceeds, the original Col_r order collapses and the cross-linking reaction stops, as shown in B. As a result, short polymers, C, break apart and dissolve in liquid paraffin. When the temperature drops, C assembles each other to form longer and thicker disc, D, which further assembles to fibrous product, E, both of which change in size depending on the cooling rate, as shown in **Fig. 3** and **Video S1**.

As noted in 2.2, the apparent reaction products of TPC1_p-12 were more linear than TPC1_p-n (n = 14, 16). In fact, its reaction proceeded more smoothly, and sometimes insoluble products were found [23]. We think faster photoreaction may be attributed to higher mobility of TPC1_p-12 molecules as the LC transition temperature is a little lower than TPC1_p-n (n = 14, 16) (**Table 1**), which allows it to react more frequently for making C longer.

3. Conclusion

The reaction of TPC1_p-n (n = 12, 14, 16), a liquid crystalline triphenylene derivative with cinnamic acid esters as photoreactive sites, with UV irradiation in liquid paraffin was carefully studied. The results show that at temperatures where the Col_r phase develops, the photoreaction afforded crescent-shaped or helical fibers, which are thermoreversible and soluble in toluene as well. Based on these results, an expected reaction mechanism was proposed in which photoirradiation is expected to result in the formation of low molecular weight poly-TPC1_p-n, which is then assembled into the fibers as an apparent product. The present results differ largely from the previously reported ones for TPC2_{mp}-n, which have two alkoxy chains in the cinnamate moiety and show a Col_h phase [23]. It has been shown that TPCs can be a new group of triphenylene derivative liquid crystals that exhibit different properties [4,7–21,24].

4. Experimental section

4.1. Measurements

The spectroscopic and thermal measurements, differential scanning calorimetry (DSC), polarized optical microscopy (POM), X-ray diffraction (XRD) measurements were the same as those reported in a previous study [23].

The thermal behavior of UV irradiated TPC1_p-n was observed using the POM apparatus with a temperature-controllable stage.

The surface morphology of UV irradiation product was observed by dynamic force mode atomic force microscopy (AFM) (SII Nanotechnology Co. Ltd, SPA300) with an SPI-3800 probe station and a silicon single-crystal cantilever (spring constant 1.4 N m⁻¹).

4.2. Synthesis

In this study, two kinds of TPC derivatives, TPC1_p-6 and TPC1_p-16 were synthesized following the procedure reported in the

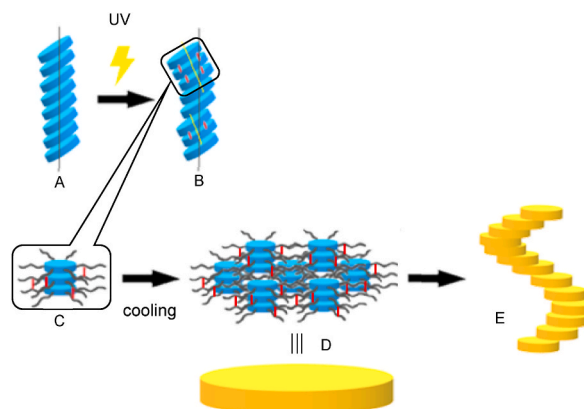


Fig. 4. Expected mechanism of formation of fibrous products by UV irradiation to triphenylene cinnamates (TPCs) in liquid paraffin.

previous study [23]. They are soluble in THF, CHCl_3 , benzene, toluene, but not in hexane.

2,3,6,7,10,11-Hexakis(*p*-hexyloxycinnamoyloxy)triphenylene **TPC1_p-6**.

Yield: 27.9 %, colorless needles.

mp: 164.5–166.5 °C; ^1H NMR (300 MHz, CDCl_3 , δ): 8.35 (s, 6H, Ar-*H*), 7.85 (d, 6H, $J = 16$ Hz, Ar-*CH*), 7.39 (d, 12H, $J = 8.7$ Hz, Ar-*H*), 6.79 (d, 12H, $J = 8.7$ Hz, Ar-*H*), 6.48 (d, 6H, $J = 16$ Hz, - CHCO_2Ar), 3.94 (t, 12H, $J = 6.8$ Hz, - $\text{OCH}_2\text{C}_5\text{H}_{11}$), 1.78 (quint, 12H, $J = 6.8$ Hz, - $\text{OCH}_2\text{CH}_2\text{C}_4\text{H}_9$), 1.52–1.40 (m, 12H, - $\text{OC}_2\text{H}_4\text{CH}_2\text{C}_3\text{H}_7$), 1.40–1.29 (m, 24H, - $\text{OC}_3\text{H}_6\text{C}_2\text{H}_4\text{CH}_3$), 0.91 (t, 18H, $J = 6.8$ Hz, - $\text{OC}_5\text{H}_{10}\text{CH}_3$); ^{13}C NMR (125 MHz, CDCl_3 , δ): 164.8, 161.1, 146.8, 142.3, 130.0, 127.5, 126.6, 118.5, 114.7, 113.9, 68.1, 31.6, 29.2, 25.7, 22.6, 14.0; IR (KBr): $\nu = 2930, 2858, 1737, 1633, 1604, 1511, 1421, 1236, 1201, 1173, 1129, 825$ cm^{-1} ; MALDI-TOF (m/z): [**TPC1_p-6**+Na] $^+$ $\text{C}_{108}\text{H}_{120}\text{O}_{18}\text{Na}$ calcd. 1727.837; found 1727.939 [**M**+Na] $^+$, 1728.944 [**M**+1+Na] $^+$, 1729.881 [**M**+2+Na] $^+$.

2,3,6,7,10,11-Hexakis(*p*-hexadecyloxycinnamoyloxy)triphenylene **TPC1_p-16**.

Yield: 42.4 %, pale brown wax.

^1H NMR (300 MHz, CDCl_3 , δ): 8.32 (s, 6H, Ar-*H*), 7.84 (d, 6H, $J = 16$ Hz, Ar-*CH*), 7.37 (d, 12H, $J = 8.6$ Hz, Ar-*H*), 6.81 (d, 12H, $J = 8.6$ Hz, Ar-*H*), 6.47 (d, 6H, $J = 16$ Hz, - CHCO_2Ar), 3.93 (t, 12H, $J = 6.7$ Hz, - $\text{OCH}_2\text{C}_{15}\text{H}_{31}$), 1.77 (quint, 12H, $J = 6.7$ Hz, - $\text{OCH}_2\text{CH}_2\text{C}_{14}\text{H}_{29}$), 1.51–1.39 (m, 12H, - $\text{OC}_2\text{H}_4\text{CH}_2\text{C}_{13}\text{H}_{27}$), 1.39–1.19 (m, 144H, - $\text{OC}_3\text{H}_6\text{C}_{12}\text{H}_{24}\text{CH}_3$), 0.88 (t, 18H, $J = 6.7$ Hz, - $\text{OC}_{15}\text{H}_{30}\text{CH}_3$); ^{13}C NMR (125 MHz, CDCl_3 , δ): 165.9, 162.1, 147.7, 143.3, 131.1, 128.5, 127.7, 119.5, 115.7, 115.1, 69.2, 33.0, 30.8, 30.7, 30.6, 30.5, 30.3, 27.1, 23.8, 15.2; IR (KBr): $\nu = 2921, 2851, 1730, 1633, 1604, 1510, 1421, 1238, 1203, 1174, 1130, 825$ cm^{-1} ; MALDI-TOF (m/z): [**TPC1_p-16**+Na] $^+$ $\text{C}_{168}\text{H}_{240}\text{O}_{18}\text{Na}$ calcd. 2568.776; found 2568.599 [**M**+Na] $^+$, 2569.647 [**M**+1+Na] $^+$, 2570.657 [**M**+2+Na] $^+$, 2571.652 [**M**+3+Na] $^+$.

4.3. Helical fiber preparation

The fiber preparation method was the same that reported in the previous study [23]. Occasionally a long UV irradiation time of up to 72 h was applied.

Data availability statement

Data will be made available on request.

CRedit authorship contribution statement

Takuji Hirose: Writing – original draft, Supervision, Project administration, Formal analysis, Conceptualization. **Yuka Kikuchi**: Investigation. **Tomoaki Nakano**: Investigation. **Tsukasa Ohno**: Investigation. **Kengo Kawamura**: Investigation. **Normazliana Binti Nazri**: Investigation. **Atsuhiko Fujimori**: Resources. **Koichi Kodama**: Writing – review & editing, Formal analysis. **Mikio Yasutake**: Investigation, Formal analysis.

Declaration of competing interest

The authors declare that they have no known competing financial interests or personal relationships that could have appeared to influence the work reported in this paper.

Acknowledgments

The authors acknowledge Mr. Hiroki Machida (Present affiliation: Achilles Corporation) for his assistance in AFM measurements. Takuji Hirose thanks Prof. Bruce W. Baldwin of Spring Arbor University for his discussion. We would like to thank Editage (www.editage.com) for English language editing.

Appendix A. Supplementary data

Supplementary data to this article can be found online at <https://doi.org/10.1016/j.heliyon.2023.e22037>.

References

- [1] Special issue on supramolecular chemistry and self-assembly, *Science* 295 (2002) 2395–2421.
- [2] T. Kato, N. Mizoshita, K. Kishimoto, *Angew. Chem. Int. Ed.* 45 (2006) 38–68.
- [3] J.G. Rudick, V. Percec, *Acc. Chem. Res.* 41 (2008) 1641–1652.
- [4] M. Kumar, S. Varshney, S. Kumar, *Polym. J.* 53 (2021) 283–297.
- [5] E.-K. Fleischmann, R. Zentel, *Angew. Chem. Int. Ed.* 52 (2013) 8810–8827.
- [6] S.I. Stupp, L.C. Palmer, *Chem. Mater.* 26 (2014) 507–518.
- [7] T. Kato, J. Uchida, T. Ichikawa, T. Sakamoto, *Angew. Chem. Int. Ed.* 57 (2018) 4355–4371.
- [8] Y. Ishida, H. Sakata, A.S. Achalkumar, K. Yamada, Y. Matsuoka, N. Iwahashi, S. Amano, K. Saigo, *Chem. Eur. J.* 17 (2011), 14752–14672.

- [9] M. Amorín, A. Pérez, J. Barberá, H.L. Ozores, J.L. Serrano, J.R. Granja, T. Sierra, *Chem. Commun.* 50 (2014) 688–690.
- [10] K. Takenami, S. Uemura, M. Funahashi, *RSC Adv.* 6 (2016) 5474–5484.
- [11] M. Gupta, Y. Suzuki, T. Sakamoto, M. Yoshio, S. Torii, H. Katayama, T. Kato, *ACS Macro Lett.* 8 (2019) 1303–1308.
- [12] D.-G. Kang, M. Park, D.-Y. Kim, M. Goh, N. Kim, K.-U. Jeong, *ACS Appl. Mater. Interfaces* 8 (2016) 30492–30501.
- [13] T. Wöhrle, I. Wurzbach, J. Kirres, A. Kostidou, N. Kapernaum, J. Litterscheidt, J.C. Haenle, P. Staffeld, A. Baro, F. Giesselmann, S. Laschat, *Chem. Rev.* 116 (2016) 1139–1241.
- [14] M. Kumar, S. Kumar, *Polymer J* 49 (2017) 85–111.
- [15] J.P. Hill, W. Jin, A. Kosaka, T. Fukushima, H. Ichihara, T. Shimomura, K. Ito, T. Hashizume, N. Ishii, T. Aida, *Science* 304 (2004) 1481–1483.
- [16] H. Iino, J. Hanna, *Jpn. J. Appl. Phys.* 45 (2006) L867.
- [17] M. Yoshio, T. Kagata, K. Hoshino, T. Mukai, H. Ohno, T. Kato, *J. Am. Chem. Soc.* 128 (2006) 5570–5577.
- [18] J.H. Park, K.H. Kim, Y.W. Park, J.P.F. Lagerwall, G. Scalia, *Langmuir* 31 (2015) 9432–9440.
- [19] D.-G. Kang, D.-Y. Kim, M. Park, Y.-J. Choi, P. Im, J.-H. Lee, S.-W. Kang, K.-U. Jeong, *Macromolecules* 48 (2015) 898–907.
- [20] S. Bhattacharjee, J.A.M. Lugger, R.P. Sijbesma, *Macromolecules* 50 (2017) 2777–2783.
- [21] Z. Zhang, H. Yang, A. Zhang, J. Bi, Y. Feng, W. Zhang, C. Zhang, J. Pu, *J. Mater. Chem. C* 6 (2018) 5597–5600.
- [22] Y. Shoji, M. Kobayashi, A. Kosaka, R. Haruki, R. Kumai, S. Adachi, T. Kajitani T. Fukushima, *Chem. Sci.* 13 (2022) 9891–9901.
- [23] T. Hirose, Z. Xu, Y. Kikuchi, M. Fukushima, K. Kawamura, Y. Kaguchi, K. Kodama, M. Yasutake, *J. Polym. Sci., Part A: Polym. Chem.* 57 (2019) 605–612.
- [24] S. Laschat, A. Baro, N. Steinke, F. Giesselmann, C. Hägele, G. Scalia, R. Judele, E. Kapatsina, S. Sauer, A. Schreivogel, M. Tosoni, *Angew. Chem. Int. Ed.* 46 (2007) 4832–4887.